JOURNAL OF MATERIALS SCIENCE 31 (1996) 2551–2556

Crystal structure and dielectric properties of $(Pb_{1-x}Ca_x)(Zr_{1-y}Sn_y)O_3$ ceramics

TAE-SERK CHUNG, HO-GI KIM
Department of Materials Science & Engineering, Korea Advanced Institute of Science & Technology, 373-1 Kusong-dong Yusong-gu Taejon 305-701 Korea

There has been an increasing demand for dielectric resonator materials that operate in the microwave frequency range for applications in microwave communications. (Pb,Ca)ZrO_3 ceramics have a dielectric constant (ε_r), high quality factor (Q) and a small temperature coefficient of resonant frequency (τ_f). However, basic properties such as its crystal structure, temperature characteristics and the nature of its phase transformation are not yet fully understood. The temperature coefficient of resonant frequency can be controlled fairly well with the temperature coefficient of the dielectric constant. In this paper, we report the results of investigated crystal structure and the dielectric properties of $(Pb_{1-x}Ca_x)(Zr_{1-y}Sn_y)O_3$ ceramics with the objective of elucidating the relationship between the crystal structure and the dielectric properties. The crystal structure refinement was performed by the Rietveld method. The dielectric properties were measured from −150–350 °C. The phase transformation was analysed from high and low temperature XRD data.

1. Introduction

In the development of telecommunications and high frequency integrated circuits, various microwave ceramic dielectrics have been used in band-pass filters, resonators and amplifiers. For microwave applications, ceramic dielectrics should satisfy the requirements of high ε_r, high Q and small τ_f. A high ε_r means that the components can be miniaturized. Thus there is considerable interest in developing high dielectric constant materials for microwave use. Because most ceramic dielectrics obey the empirical relation [1, 2] $\tau_f = -\tau_\varepsilon/2 + \alpha_1$, τ_ε should be around 10–20 p.p.m. $°C^{-1}$ in order to make τ_f 0 p.p.m. $°C^{-1}$ (in most ceramic dielectrics α_1 is 5–10 p.p.m. $°C^{-1}$). In general, high ε_r ceramic dielectrics have a large negative value of τ_ε. So, τ_f has a high positive value. However, microwave ceramic dielectrics almost have a new 0 p.p.m. $°C^{-1}$ for τ_f. This result is caused by a positive τ_ε arising from a phase transformation. Therefore, the transition temperature effectively controls τ_f as well as τ_ε. (Pb,Ca)ZrO_3 ceramics (PCZ), as reported by Kato *et al.* [3], have a high dielectric constant, high quality factor and a small τ_f in the microwave range. Also τ_f can be changed from positive to negative in the composition range Pb:Ca = 7:3–6:4. The crystal structure and nature of the phase transformation in this system has not been clearly identified. In order to investigate the phase transformation through dielectric measurements, an impedance analyser HP-4192A was used because the dielectric constant in the microwave range was not significantly different from the one at 1 MHz. We have measured the high and low temperature behaviour of ε_r together with a crystal structure analysis in order to analyse the phase transformation of $(Pb_{1-x}Ca_x)(Zr_{1-y}Sn_y)O_3$ ceramics (PCZS).

The dielectric properties have a close relationship with the crystal structure in ceramic dielectrics. In the PCZ system, the crystal structure proposed as being rhombohedral, space group R3c in the range (Pb:Ca = 7:3 ~ 6:4) [4]. In our XRD experiments, however, we could not get satisfactory results using this space group. To find out the correct unit cell structure, XRD simulations using various unit cells were performed. The crystal structure refinement was performed using the Rietveld method [5] which can be applied to powder X-ray diffraction data. In addition the change in lattice parameters with the degree of Sn substitution was investigated.

2. Experimental procedure

The reagents were PbO, $CaCO_3$, ZrO_2, and SnO_2 with purities over 99.9%. In the series $(Pb_{1-x}Ca_x)(Zr_{1-y}Sn_y)O_3$, the compositions were $x = 0.3$, 0.325, 0.35, 0.375 and $y = 0$, 0.1, 0.2, 0.3. The powder preparation was done by the conventional mixed-oxide method. In order to minimize the vaporization of PbO, $PbZrO_3$ was synthesized and then used along with a 1 wt % excess of PbO in the starting powder. The powder was mixed for 18 h in a ball mill in distilled water with calcia-stabilized ZrO_2 balls. The mixed powder was calcined at 850 °C for 3 h. The calcined powder was ball-milled for 18 h in acetone. The powder with 1 wt % PVA binder was pressed (89 MPa) into a pellet. Sintering was performed

0022–2461

under an atmosphere generated from powders of $PbZrO_3$ + 10 wt % ZrO_2 in a sealed Al_2O_3 crucible. The sintering conditions were 1250, 1300, 1350 and 1400 °C for 2 h. To identify the optimum sintering condition, density measurements were performed using the Archimedes technique. The final sintering conditions were chosen to be 1300 °C, for 2 h because all compositions were over 95% of the theoretical density. Silver paste was used for the electrodes on the sintered specimen. Powders for XRD were prepared by grinding the sintered specimens and further annealing at 700 °C for 3 h to minimize residual stress and thus any stress-induced phase transformation. For the Rietveld analysis, the X-ray data were obtained using the step scanning method with a 0.02° step. The patterns were recorded between 2θ angles 20°–100°. The beam was monochromated using a curved graphite monochromator. The crystal structure refinement was performed by using the program DBWS-9411 [6]. High and low temperature X-ray diffraction patterns were collected at −183, 350 and 700 °C.

The dielectric characteristics were measured from 25–400 °C and from −150–25 °C with a HP-4192A impedance analyser operating at a measuring frequency of 1 MHz. A schematic representation of the experimental apparatus used for the low temperature measurements is presented in Fig. 1.

3. Results and discussion

3.1. Crystal structure analysis

The X-ray diffraction patterns of PCZS are shown in Fig. 2. Kato *et al.* reported that the PCZ system has a rhombohedral structure with a R3c space group [4]. The rhombohedral assignment was apparently verified by the observation of the splitting of the (1 1 1), (1 1 $\bar{1}$) peaks and the (2 2 2), (2 2 $\bar{2}$) peaks which is characteristic of this symmetry. However a difficulty was experienced in calculating the lattice constants and this was reflected in the large standard deviations of the fitted parameters. In addition the peak profiles were different from those expected from a rhombohedral structure. If the unit cell structure is rhombohedral, then two conditions exist namely $\alpha < 90°$ and $\alpha > 90°$. This means that there are differences in the multiplicity between the (2 2 2) and (2 2 $\bar{2}$) peaks as are listed in Table I. These differences result in very different diffraction intensities. The simulated XRD patterns and the measured XRD patterns are shown in Fig. 3a. The measured XRD pattern does not coincide with either of the simulated ones. We believe this is because the calculations have been performed using the wrong unit cell. We have simulated the XRD pattern using an orthorhombic unit cell constructed with a special monoclinic *b*-setting lattice with $a = b = c$, $\beta < 90°$ as shown in Fig. 4. The measured and the simulated XRD patterns are shown in Fig. 3b. As can be seen there is good agreement between the experimental and simulated patterns. Superlattice peaks can be identified in Fig. 5. The indexing of these superlattice peaks listed in Table II suggests that the unit cell parameters should be doubled. From various simulations, it was discovered that the superlattice was created by the tilting of oxygen ions rather than the ordering of the A-site ions of Pb^{2+} and Ca^{2+}. Considering these results and applying the extinction rules of (Table III), the space group of $(Pb_{0.7}Ca_{0.3})ZrO_3$ was assigned to be orthorhombic space group Cmmm. The crystal structure refinement by the Rietveld method was completed at $R_{wp} = 9.78\%$, $R_{exp} = 2.47\%$ (Table IV, Fig. 6). The definition of R_{exp} is presented in Equation 1 [6]. The refined lattice parameters were $a = 1.1622$ nm, $b = 1.1551$ nm and $c = 0.8191$ nm.

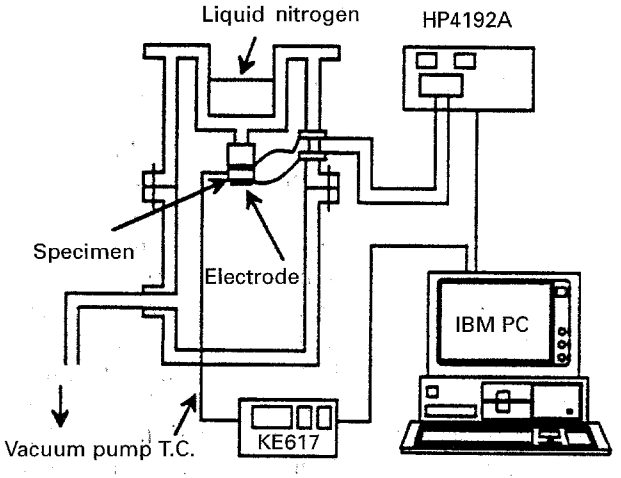

Figure 1 Measurement system for low temperature dielectric properties.

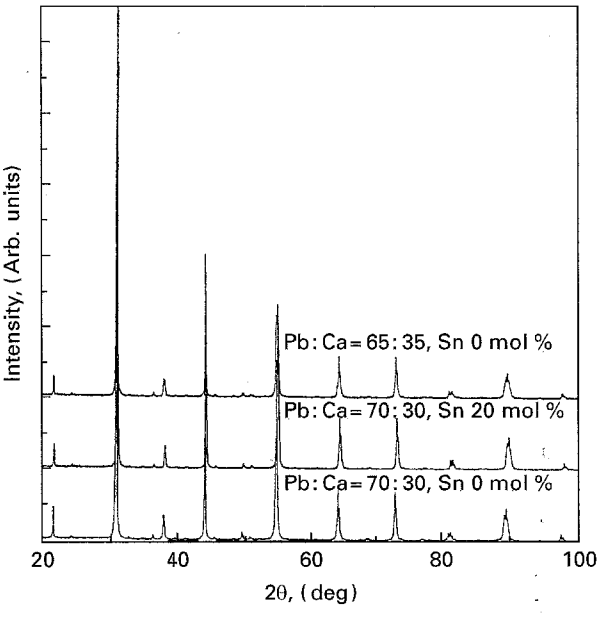

Figure 2 XRD pattern of $(Pb_{1-x}Ca_x)(Zr_{1-y}Sn_y)O_3$ system sintered at 1300 °C for 2 h.

TABLE I Multiplicities of diffraction planes in rhombohedral unit cell

Planes	Multiplicity ($\alpha > 90°$)	Multiplicity ($\alpha < 90°$)
(2 2 2)	8	2
(2 2 $\bar{2}$)	2	8

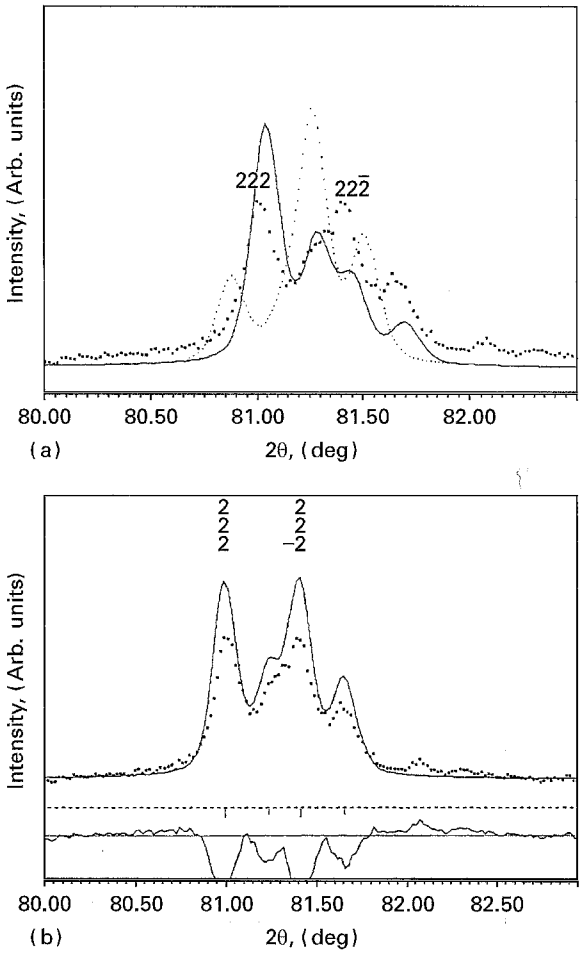

Figure 3 Measured and simulated XRD pattern for $(Pb_{0.7}Ca_{0.3})ZrO_3$ based on (a) rhombohedral unit cell, (■ ■ ■) measured, (—) simulated for $\alpha > 90°$ (· · · ·) simulated for $\alpha < 90°$ and (b) monoclinic unit cell, (■ ■ ■) measured and (—) simulated.

$$R_{exp} = \left[\frac{N - P + C)}{\Sigma w_i y_i^2}\right]^{\frac{1}{2}}$$

N: Number of data points
P: Number of parameters adjusted
C: Number of constraints
w_i: Weighting factor
y_i: Measured intensity (1)

The low value of R_{exp} is caused by the extremely high scattering intensity of the Bragg reflections (use of self-rotating-anode type diffractometer). This also means results in a large value of the S parameter $(= R_{exp}/R_{exp})$ which can only be minimized by the choice of the exact space group.

3.2. Dielectric properties

To investigate the temperature characteristics of the dielectric constant, an experimental capacitance was measured and normalized with respect to the capacitance at 30 °C as is shown in Figs 7 and 8. The tan δ was lower than 1% in all compositions. Various phase transformations were observed in the PCZS system as a function of temperature. Low temperature phase transformations in $Pb_{0.65}Ca_{0.35}ZrO_3$ were observed at − 10 °C as is shown in Fig. 9 and also at − 183 °C. The high temperature phase transition can

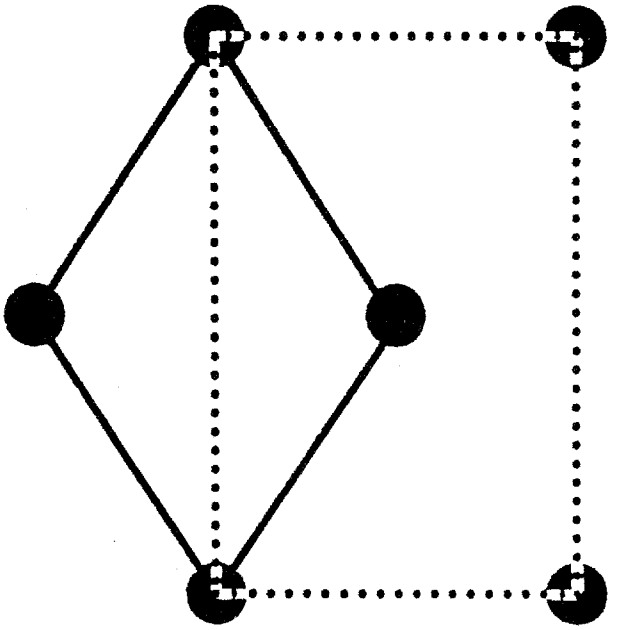

Figure 4 Monoclinic to orthorhombic unit cell transformation. (—) Monoclinic b setting (0 1 0) and (- - - -) orthorhombic setting (0 0 1).

TABLE II Superlattice peak index based on monoclinic unit cell

2θ (deg)	d (nm)	Index
24.181	0.36805	0 1/2 1
32.619	0.27452	1/2 1 1
34.561	0.25952	0 1/2 3/2
36.322	0.24733	1/2 3/2 1/2
39.552	0.22785	1 0 3/2
41.133	0.21945	1 1/2 3/2
45.526	0.19924	1 1 3/2
48.325	0.18834	1/2 3/2 3/2
50.847	0.17957	1/2 1 2

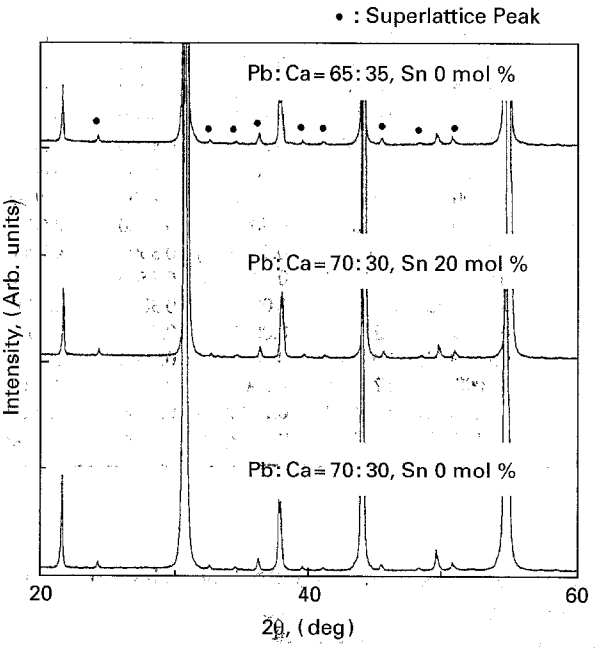

Figure 5 XRD patterns of $(Pb_{1-x}Ca_x)(Zr_{1-y}Sn_y)O_3$ system.

be found between 100 °C and 300 °C. These types of phase transformation can be denoted as 'H' for high temperature and 'L' for low temperature. The $Pb_{0.65}Ca_{0.35}ZrO_3$ 'H' type transformation at about

TABLE III Extinction rules for the C_{mmm} space group

Reflection	Conditions
hkl	h + k
0kl	k
h0l	h
hk0	h + k
h00	h
k00	k

TABLE IV (a) Summary of the Structure Refinement for $(Pb_{0.7}Ca_{0.3})ZrO_3$ at room temperature. With e.s.d.'s in parentheses; CuK_α radiation, $\lambda = 0.1540598$ nm

Space group	C_{mmm}
a (nm)	1.16218(3)
b (nm)	1.15508(3)
c (nm)	0.81914(2)
α (deg)	90.0
β (deg)	90.0
γ (deg)	90.0
Pattern 2θ range (deg)	20.02–100.0
Step angle (deg)	0.02
Number of steps	4000
R_{wp} (%)	9.78
R_p (%)	7.36
R_{exp} (%)	2.47

TABLE IV (b) Fractional atomic coordinates and isotropic thermal parameters. U_{iso} (nm) with e.s.d.'s in parentheses

ATOM	*X*	*Y*	*Z*	U_{iso} $\times 10^{-1}$ nm	*N*
PB1	0.0000	0.0000	0.0000	0.9000	0.6547
CA1	0.0000	0.0000	0.0000	0.5000	0.3000
PB2	0.5000	0.0000	0.0000	0.9000	0.6547
CA2	0.5000	0.0000	0.0000	0.5000	0.3000
PB3	0.0000	0.0000	0.5000	0.9000	0.6547
CA3	0.0000	0.0000	0.5000	0.5000	0.3000
PB4	0.5000	0.0000	0.5000	0.9000	0.6547
CA4	0.5000	0.0000	0.5000	0.5000	0.3000
PB5	0.2500	0.2500	0.0000	0.9000	1.3095
CA5	0.2500	0.2500	0.0000	0.5000	0.6000
PB6	0.2500	0.2500	0.5000	0.9000	1.3095
CA6	0.2500	0.2500	0.5000	0.5000	0.6000
ZR1	0.2436(6)	0.0000	0.2603(13)	0.3500	4.0000
ZR2	0.0000	0.2576(5)	0.2442(13)	0.3500	4.0000
01	0.1676(52)	0.0000	0.0000	0.3000	2.0000
02	0.0000	0.2174(57)	0.0000	0.3000	2.0000
03	0.2196(54)	0.0000	0.5000	0.3000	2.0000
04	0.0000	0.2359(58)	0.5000	0.3000	2.0000
05	0.1048(23)	0.1214(28)	0.1733(30)	0.3000	8.0000
06	0.1177(29)	0.3939(23)	0.2698(38)	0.3000	8.0000

200 °C was investigated at 350 °C by high temperature XRD techniques and a cubic structure pattern was observed as shown in Fig. 10b. Even at this temperature, superlattice peaks were still observed. Absence of these superlattice peaks was observed in the XRD pattern at 700 °C as is shown in Fig. 10c. From this result, there may be another phase transition between 350 °C and 700 °C. But its transformation temperature cannot be correlated with a dielectric constant

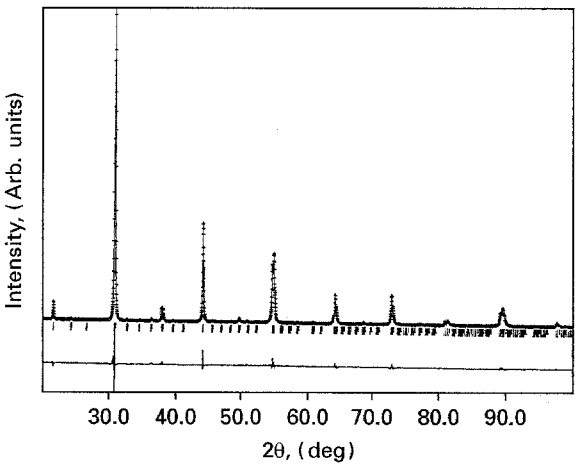

Figure 6 Observed and calculated XRD pattern of $(Pb_{0.7}Ca_{0.3})ZrO_3$ (orthorhombic, Cmmm space group).

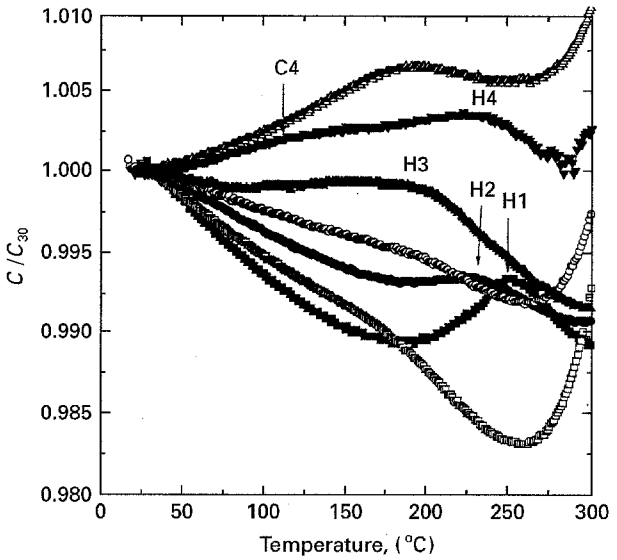

Figure 7 Temperature characteristics of the $(Pb_{1-x}Ca_x)(Zr_{1-y}Sn_y)O_3$ system (30–350 °C). (–■–) $x = 0.3$, $y = 0$, (–□–) $x = 0.3$, $y = 0.2$, (–●–) $x = 0.325$, $y = 0$, (–○–) $x = 0.325$, $y = 0.2$, (–▲–) $x = 0.35$, $y = 0$, (–△–) $x = 0.35$, $y = 0.2$, (–▼–) $x = 0.375$, $y = 0$.

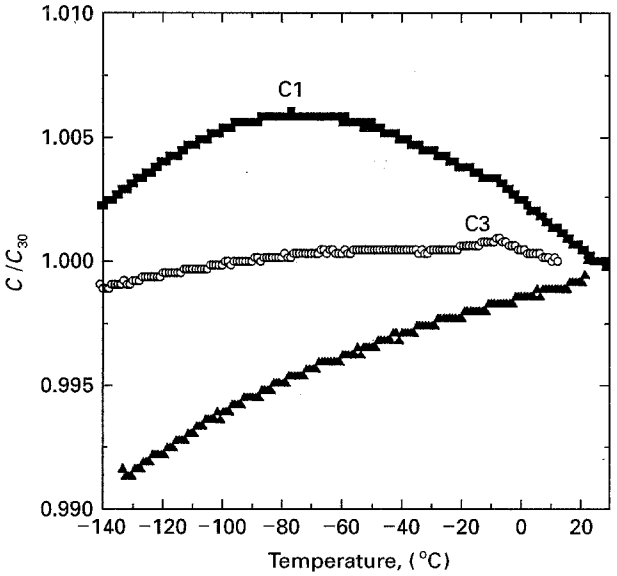

Figure 8 Temperature characteristics of the $(Pb_{1-x}Ca_x)ZrO_3$ system (−140–30 °C). (–■–) $x = 0.3$, (–○–) $x = 0.35$ and (–▲–) $x = 0.38$.

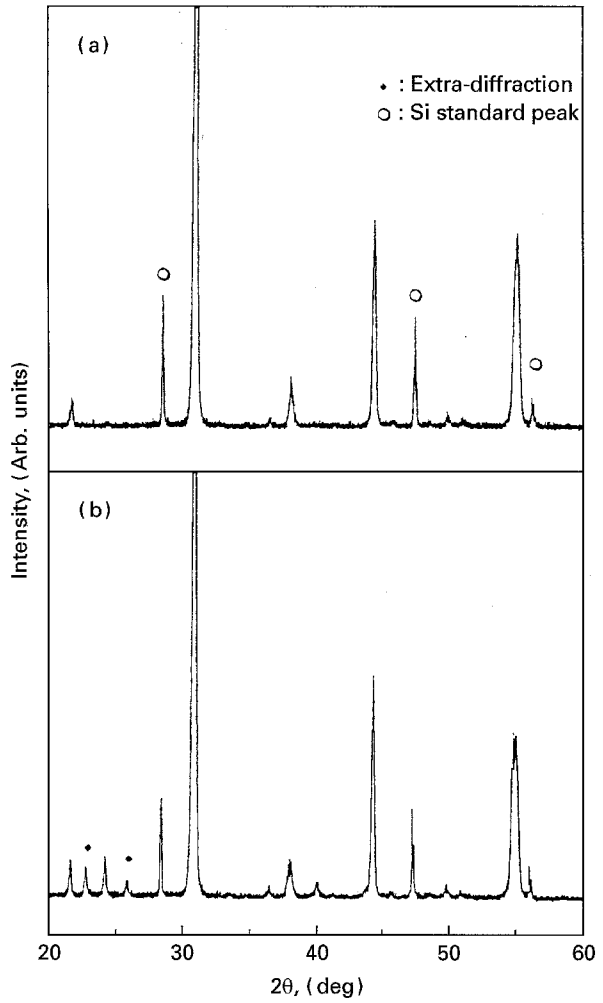

Figure 9 XRD patterns of $(Pb_{0.65}Ca_{0.35})ZrO_3$ at (a) 30 °C and (b) −183 °C.

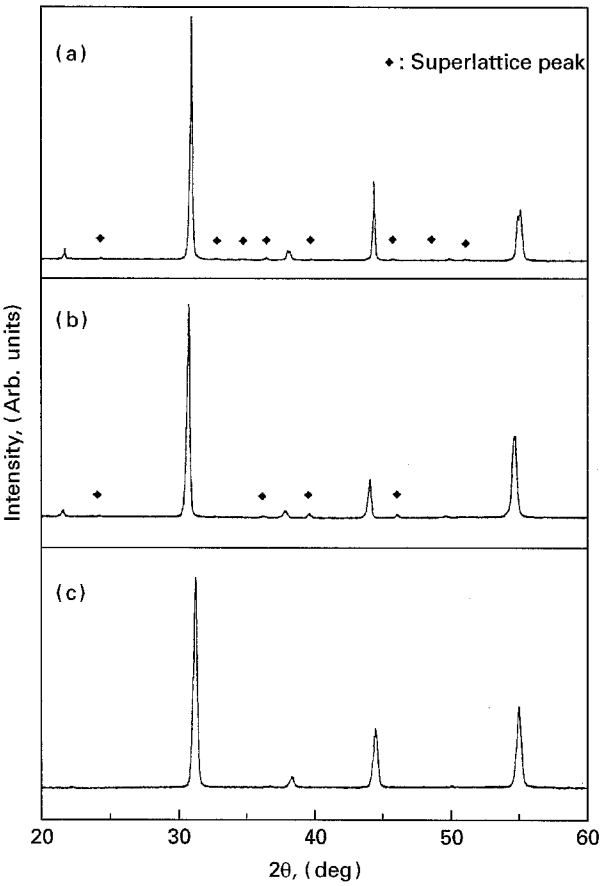

Figure 10 XRD patterns of $(Pb_{0.65}Ca_{0.35})ZrO_3$ at (a) 30 °C, (b) 350 °C and (c) 700 °C.

TABLE V Lattice parameters (in nm) of (C_{mmm}) of $(Pb_{0.7}Ca_{0.3})Zr_{1-x}Sn_xO_3$. (Orthorhombic unit cell, C_{mmm} space group)

Sn mol %	0	10	20	30
HKL	2θ			
800	63.958	64.119	64.254	64.342
444	64.168	64.306	64.432	64.517
080	64.36	64.499	64.616	64.691
662	72.899	73.084	73.189	73.3
480	73.036	73.199	73.34	73.42
804	81.013	81.203	81.379	81.518
084	81.412	81.577	81.737	81.841
a	1.1616	1.1597	1.1577	1.15598
b	1.1549	1.15333	1.15164	1.15038
c	0.819	0.818	0.8166	0.8155
b/a	0.99423	0.994507	0.994765	0.995156
c/a	0.70506	0.705355	0.705364	0.705462

measurement due to the increase of electrical conductivity at those high temperatures.

The dielectric constant decreased as the Ca and Sn content increased. A similar result was reported by Kato *et al.* [7]. The dielectric constant decrease can be explained in terms of a smaller ionic polarizability for Ca^{2+} and Sn^{4+} compared to that of the Pb^{2+} and Zr^{4+} ions [8].

With increasing Ca substitution in the PCZ system, there is no pronounced difference in the 'H' type phase transition temperature, but the 'L' type phase transition temperature increased drastically. Finally, the 'H' type and 'L' type phase transition temperature approached each other. Thus, increasing the Ca substitution makes a more positive temperature coefficient of the dielectric constant in the applications temperature range of −25 °C to 80 °C.

The Sn substitution tends to decrease the 'H' type phase transition temperature. Because the 'H' type transition is an orthorhombic to cubic phase transition, the transition temperature can be related to the amount of octahedral distortion. The lattice parameter variations are shown in Table V. The values of c/a and b/a approached 1 and $1/\sqrt{2}$ respectively as the degree of Sn substitution increased. The tendency to a cubic-like phase may be the cause of the transition temperature decrease. According to Raves [9], the variation of the Curie-temperature in a ferroelectric phase is related to octahedral distortion, with more distorted structure having a higher T_c. The octahedral distortions are related to the degree of π bonding between the B site cation and oxygen ions. Unlike the Zr^{4+} ion, the Sn^{4+} ion has no unfilled *d* orbital to make π(B–O) bonding. Thus the weakened π(B–O) bonding tends to create a more cubic-like structure. This could be the cause of the 'H' type transition temperature decrease. As a result of the transition temperature decrease, the temperature coefficient of the dielectric constant increases more positively in the temperature range for applications.

4. Conclusions

(i) The crystal structure of the $(Pb_{0.7}Ca_{0.3})ZrO_3$ ceramic was determined by the Rietveld refinement of X-ray data and found to possess the orthorhombic space group C_{mmm}.

(ii) The dielectric constant was decreased by the Ca, and Sn substitution. This could be understood in terms of the smaller ionic polarizability of Ca^{2+} and Sn^{4+} compared to that of Pb^{2+} and Zr^{4+} ions.

(iii) In the $(Pb_{1-x}Ca_x)(Zr_{1-y}Sn_y)O_3$ system, while the Ca substitution increased the 'L' type phase transformation, the Sn substitution decreased the 'H' type phase transformation temperature because the Sn modified the $(Pb,Ca)ZrO_3$ system into a cubic-like phase.

References

1. P. J. HAROP, *J. Mater. Sci.* **4** (1969) 370.
2. A. J. BOSMAN and E. E. HAVINGA, *Phys. Rev.* **129** (1963) 1593.
3. J. KATO, H. KAGATA and K. NISHIMOTO, *Jap. J. Appl. Phys.* **30** (1991) 2343.
4. J. KATO, M. FUJII, H. KAGATA and K. NISHIMOTO, *ibid.* **32** (1993) 4356.
5. H. M. RIETVELD, *Acta. Cryst.* **22** (1967) 151.
6. R. A. YOUNG, in "The Rietveld Method" (Oxford University Press, New York, 1993) p. 22.
7. J. KATO, Proceedings of Fulrath Memorial International Symposium on Advanced Ceramics, Tokyo, August 1993 (Japanese Fulrath Pacific Award Committee, Tokyo, 1993) p. 85.
8. R. D. SHANON, *J. Appl. Phys.* **73** (1993) 348.
9. J. RAVES, *Phase Transitions* **33** (1991) 53.

Received 8 August 1995
and accepted 20 November 1995